DAPNIA/SED-1998/02
17 décembre 1998

Optical anisotropy effects in lead tungstate crystals

R. Chipaux, M. Géléoc

CEA DAPNIA/SED, Saclay, France

Abstract

The anisotropic crystal structure of lead tungstate leads to strong consequences in its optical properties and their characterization. Beyond the variation of surface reflections due to the birefringence of the material, we report the observation that part of the bulk light absorption is sensitive to the light polarization direction. This variable part varies with the quality of the crystal, and is clearly related to internal structural defects. Irradiation experiments with gamma rays or fast neutrons confirm the recent improvement of the short term resistance of this scintillator. Its long term behaviour remains identical, and acceptable for the use in high energy electromagnetic calorimetry. A polarization direction dependant induced absorption is observed, specially after high levels of radiation. Ray tracing programs in development for the simulation of the light yield in lead tungstate should take into account all these anisotropic effects.

Keywords : Lead tungstate, scintillator, radiation dammage, birefringence, refractive index.

PACS : 29.40.Mc ; 78.20.-e ; 61.80.-x.

submitted to *Journal of Physics: Condensed Matter*

1 Introduction

Lead tungstate, the scintillating material foreseen for the electromagnetic calorimeter of the CMS experiment in project at the Large Hadron Collider [1, 2], has a strongly anisotropic crystal structure, scheelite type, *I4$_1$/a*, for the stoichiometric $PbWO_4$. A lead deficient phase, $Pb_7W_8O_{32-x}$, is also reported, with a "pseudo-scheelite" structure, *P4/nnc*, [3]. This anisotropy has important consequences in crystal growth, machining, etc., as reported in [4] ; it induces also directly optical birefringence, which complicates optical characterizations, as shown in the next section. It has also indirect consequences in the optical transmission properties of the material : as shown in section 3, both initial and radiation induced absorptions are sensitive to the light polarization direction.

2 Refractive index

New measurements of the lead tungstate refractive index have been recently published by S. Baccaro and co-workers [5]. Compared to their previous published data [6] only little change is found for the ordinary index, but the accuracy of extraordinary index values is greatly improved. Thus the numerical formulæ proposed in a previous note [7] should be considered as inaccurate, especially for the extraordinary index.

Results of fit based on the new data are presented in table 1 for the Cauchy formula :

$$n = \sum_{i=0}^{m_c} \frac{n_{c_i}}{\lambda^{2i}} = n_{c_0}(1 - (\frac{\lambda_{c_1}^2}{\lambda^2})(1 - (\frac{\lambda_{c_2}^2}{\lambda^2})(1 - \cdots))) \tag{1}$$

and in table 2 for the Sellmeier law :

$$n^2 - 1 = \sum_{i=0}^{m_s} \frac{n_{s_i}^2}{1 - \frac{\lambda_{s_i}^2}{\lambda^2}} \tag{2}$$

Table 1: $PbWO_4$ index fits : parameters of the five terms Cauchy formula.

	n_{c_0}	$\lambda_{c_1}^2$ (nm^2)	$\lambda_{c_2}^2$ (nm^2)	$\lambda_{c_3}^2$ (nm^2)	$\lambda_{c_4}^2$ (nm^2)
ordinary index	2.1941	-7405.9	-177418	69434	170104
extraordinary index	2.1480	5038.0	889480	142481	66245

Table 2: $PbWO_4$ index fits : parameters of the two terms Sellmeier law ($\lambda_{s_0} = 0$).

	n_{s_0}	n_{s_1}	λ_{s_1} (nm)
ordinary index	1.5914	1.0918	270.28
extraordinary index	1.6683	0.8588	266.60

Figure 1 represents the data and its fit by the Sellmeier law, compared to the previous results.

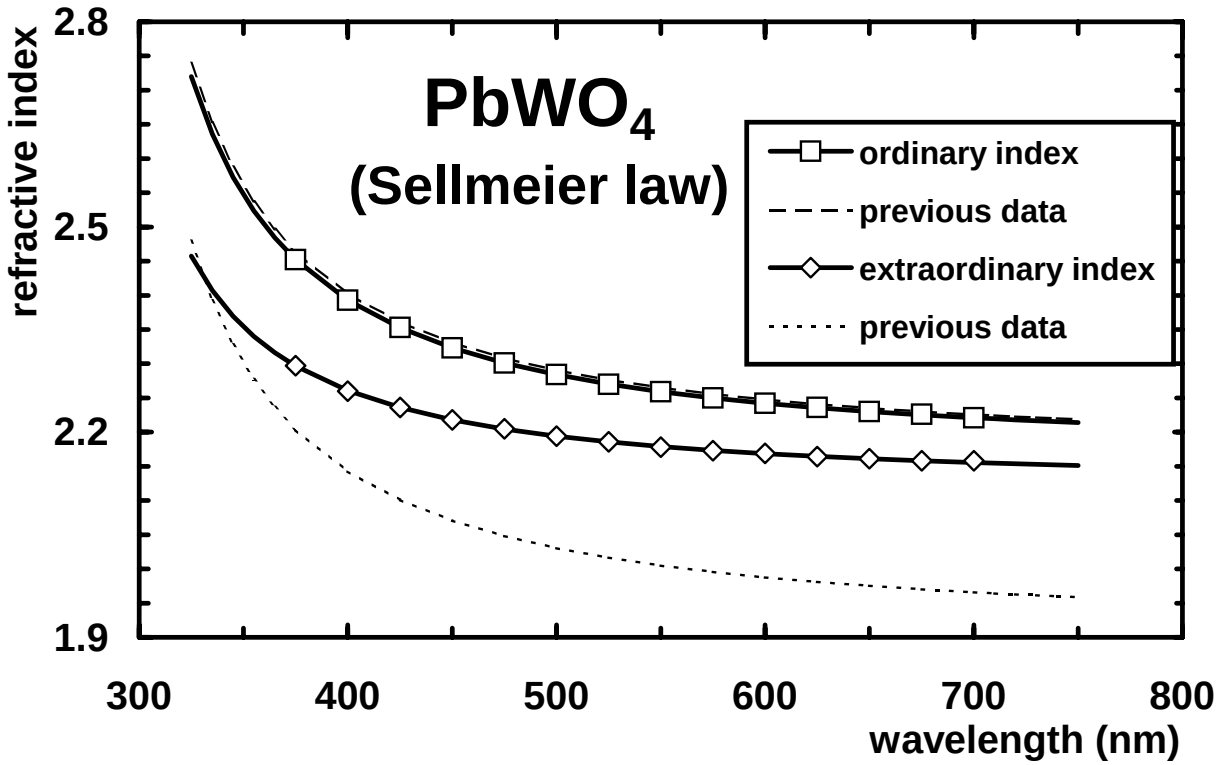

Figure 1: Ordinary and extraordinary indices of $PbWO_4$ as function of wavelength : data [5] and fit to a one term Sellmeier law ; comparison with the previous data [6, 7].

We would recommend the use of the following expressions, derived from the parameters shown in tables 1 and 2, where wavelengths λ are in nanometer :

$$n_{\mathrm{ord}} = \sqrt{3.5325 + \frac{1.19198}{1 - 73053\lambda^{-2}}} \pm 0.01 \tag{3}$$

$$n_{\mathrm{ext}} = \sqrt{3.7834 + \frac{0.73754}{1 - 71073\lambda^{-2}}} \pm 0.02 \tag{4}$$

This negative birefringence implies to take some precautions in optical transmission measurement. The intensity of the Fresnel reflections on the surface will depend on the orientation of the optical axis of the measured crystal and on the direction and polarization of the light beam. For example, at 450 nm, in the extreme case of light beams polarized perpendicularly and parallel to the optical axis, the difference in measured transmission due to this effect is 3.6 %. Taking into account this effect allowed us to put in evidence some dependencies of the optical absorption in lead tungstate with the light polarization direction, as shown in the next section.

In the recent Russian $PbWO_4$ crystals, as indicated in [4], the optical axis is parallel to the small faces and to one of the lateral faces of the crystal. It is easy to determine visually the faces traversed by the optical axis, and thus to orient the crystal in longitudinal transmission measurement in order to have, for example, the optical axis vertical. In that geometry, the light beam is perpendicular to the optical axis, and does not split in two distinct rays, and the Fresnel reflections are easily determined for any polarization state of the light beam. The simplest method would be to use linearly polarized light, either parallel or perpendicular to the optical axis and to calculate the reflections using respectively the ordinary or the extraordinary index.

3 Optical absorption

3.1 Variation with the direction of light polarization

We have performed longitudinal light transmission measurement on several Russian crystals. In this study, both sample and reference beams were polarized by UV visible linear sheet polarizers [8]. We have varied the angle θ between the direction of polarization and the optical axis from 0° to 180° (see figure 2).

An example of the set of data obtained is shown for one crystal on figure 3.

As in figure 4, we report the variations of the transmission at each wavelength and compare them to the ones that would have been induced by the modulation of the Fresnel reflections alone starting from the maximum of transmission, (*i.e.* for a direction of polarization perpendicular to the optical axis).

The amplitude of the modulation can not be always explained by the Fresnel reflections, (see for example figure 4), which indicates that part of the absorption is polarization dependent.

After correction from the reflections, we can extract the intrinsic absorption coefficient $\mu(\theta)$, which, at the first order in θ can be written as :

$$\mu(\theta) = \mu_0 + \mu_\theta \sin^2(\theta - \theta_0) \tag{5}$$

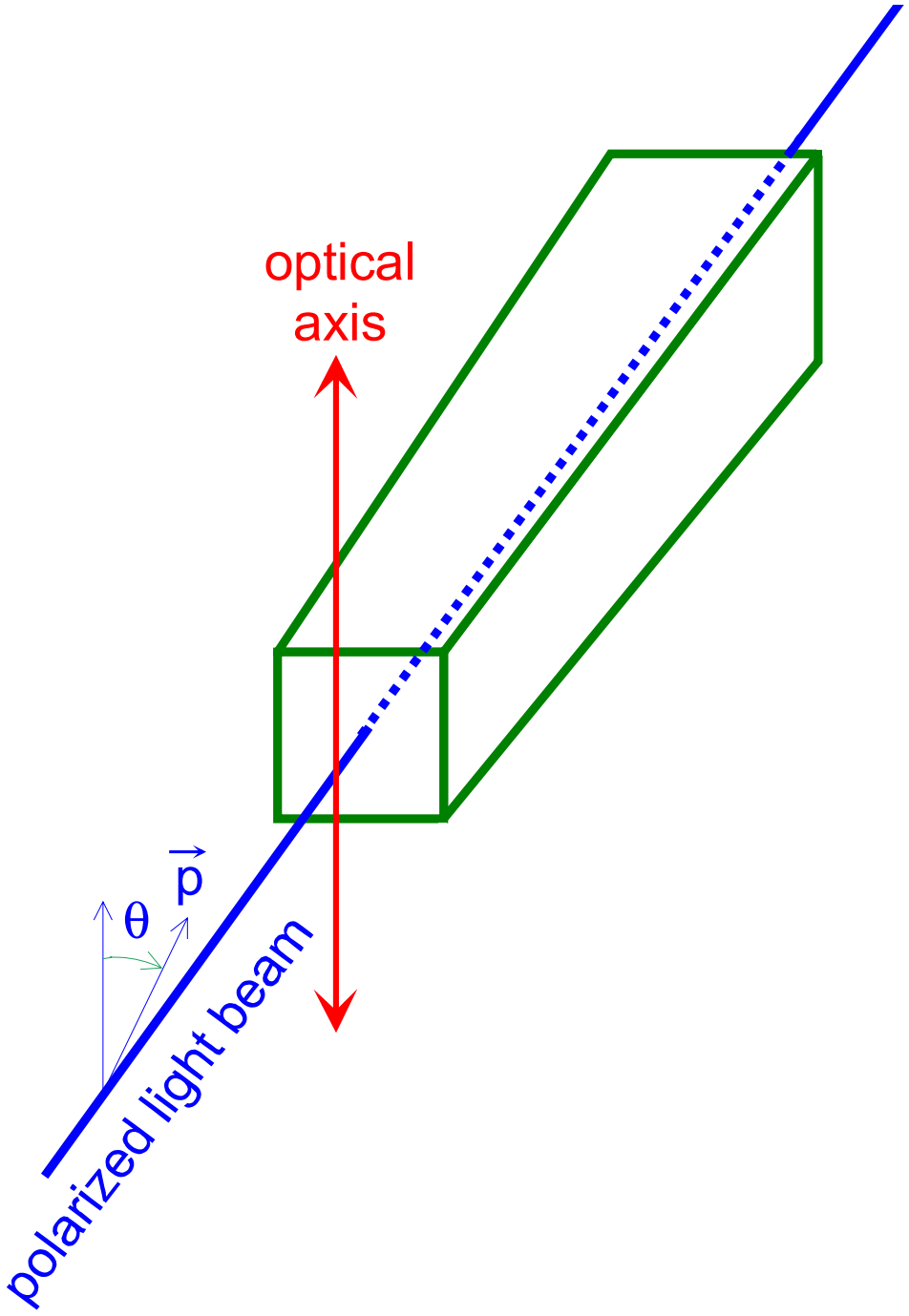

Figure 2: Scheme of the longitudinal transmission measurements.

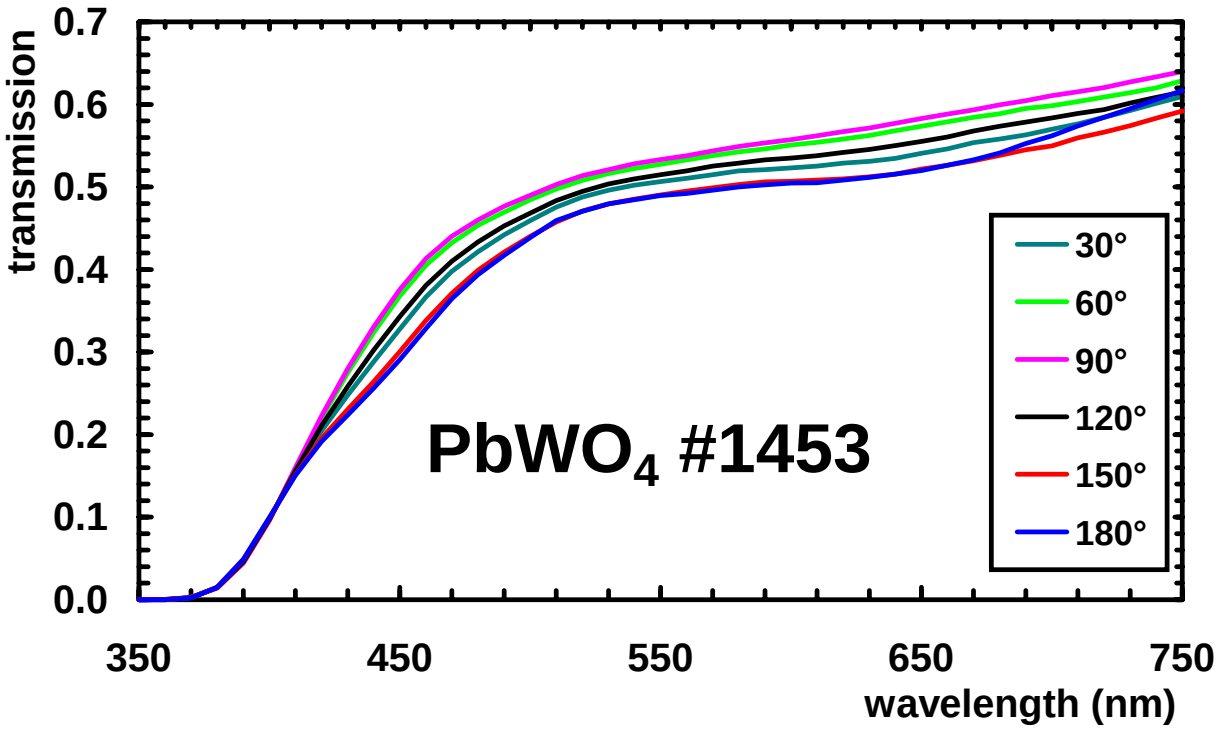

Figure 3: Longitudinal optical transmissions *versus* wavelength for crystal #1453 for different directions of the light polarization. The angle θ is the angle between the light beam and the optical axis direction.

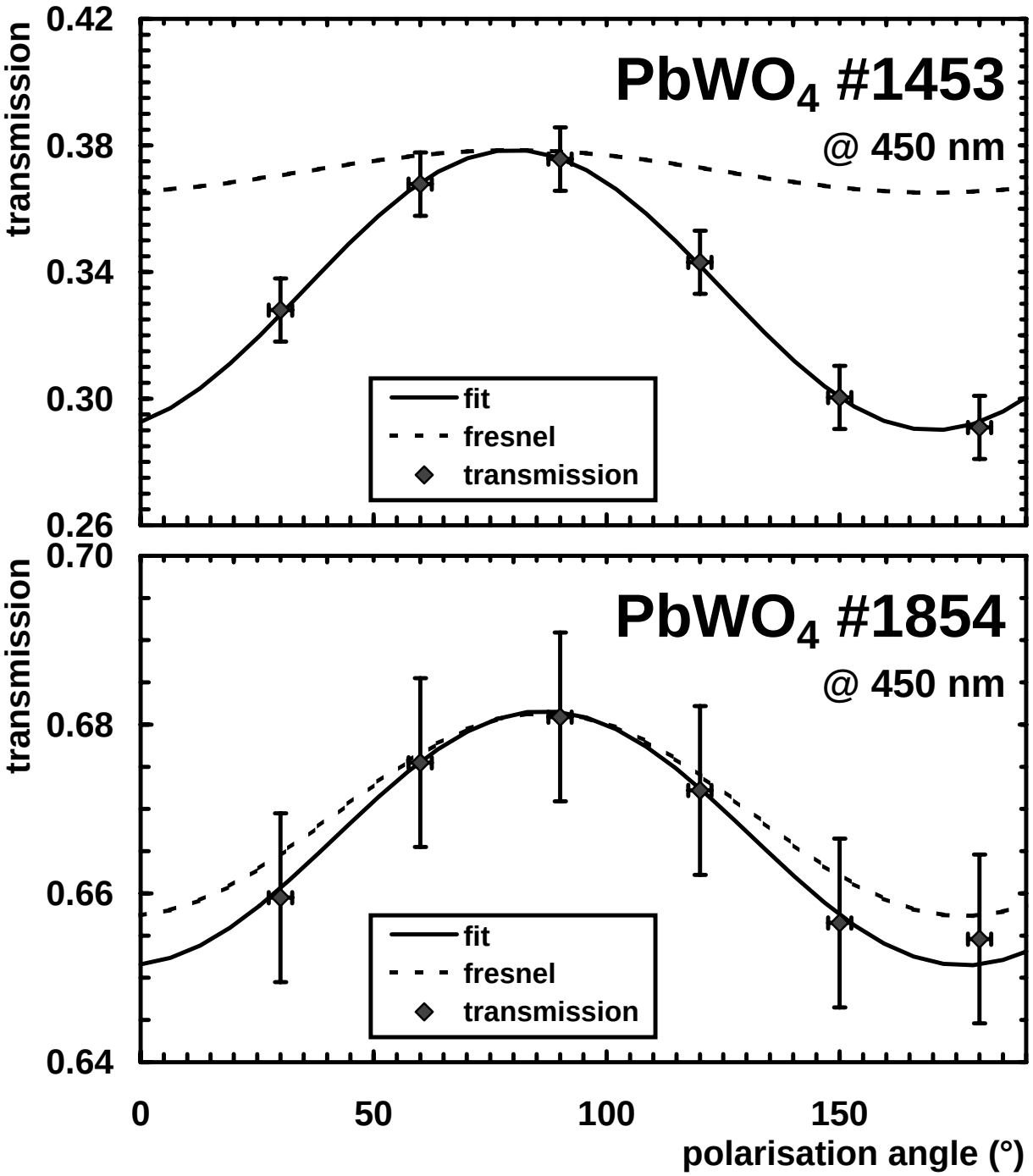

Figure 4: Transmission *versus* polarization direction for crystals #1453 and #1854 at 450 nm. Solid line : first order sinusoidal fit of the data, dashed line : modulation due to Fresnel reflections.

μ_0 is given by the maximal transmission, μ_θ and θ_0 by the amplitude and the phase of the sinusoid, corrected of the reflections. In this treatment, multiple reflections have been neglected. In all crystals, the phase of the sinusoid is independent of the wavelength, and nearly equal to 0°. The difference with 0° can be due to systematic errors caused by disorientation of the polarizer, and to little deviation of the optical axis from its ideal direction. This deviation is always below 10°, and confirm the orientation of the optical axis indicated in [4].

Figure 5 shows the variation of μ_0 and μ_θ with the wavelength. In every case, μ_θ is positive, indicating that the bulk absorption is greater when the light is polarized along the optical axis. In crystals #1453 and #1694, two bands can be observed in μ_θ, a rather sharp around 450 nm and a smaller and broader one around 650 nm. At 450 nm μ_θ can be as high as one half of μ_0. In good crystals like #1695 and #1854, μ_θ is negligible above 400 nm. In the worst crystal, #1699, no clear feature is observed in the μ_θ spectrum. In this crystal μ_θ remains almost equal to one half of μ_0 at every wavelength.

3.2 Variation under fast neutron irradiation

We have investigated the behaviour of the lanthanum doped crystal #1854 under irradiation. In a first experiment it received a gamma dose of 25 Gy at a rate of 0.5 Gy h^{-1} in our ^{60}Co irradiation facility Cocase, then in a second one it received in the reactor Ulysse a cumulated fast neutron fluence of 2 10^{14} fast neutrons cm^{-2} in three steps summarised in table 3. After annealing, a second neutron irradiation at the same fluence (2 10^{14} fast neutrons cm^{-2}) was performed. Details on the irradiation facilities have been previously published [9, 10, 11]. Transmission measurements have been performed longitudinally with light polarized linearly, parallel to the crystal optical axis (ordinary ray), or perpendicularly (extraordinary ray), after a delay of at least one week after irradiation, caused by the induced radioactivity.

The low rate gamma irradiation does not induce large degradation in the transparency as shown in figure 6. For the ordinary ray, the induced absorption coefficient remains less than 0.1 m^{-1}. These data are typical for recent rad-hard crystals. Even more, for the extraordinary ray, a small, but significant improvement is observed around 460 nm. A similar behaviour has been observed previously around 420 nm in Gd and La doped $PbWO_4$ samples [12, 13].

After annealing during 6 hours at 200° C, the initial state is practically recovered (see figure 6).

Table 3: Neutron irradiation conditions.

	fast neutrons ($E > 100$ keV) (cm^{-2})	epithermal neutrons (1 eV $< E <$ 100 keV) (cm^{-2})	thermal neutrons ($E <$ 1 eV) (cm^{-2})	ionising dose (Gy)
step 1	$1\ 10^{12}$	$3.3\ 10^{12}$	$2.9\ 10^{12}$	125
step 2	$2\ 10^{13}$	$6.7\ 10^{13}$	$5.8\ 10^{13}$	2 500
step 3	$2\ 10^{14}$	$6.7\ 10^{14}$	$5.8\ 10^{14}$	25 000

The first neutron irradiation gives results comparable to the gamma irradiation. Higher fluence induces absorption coefficients which remains less than 1 m^{-1} after 2 10^{14} fast neutrons cm^{-2}, but are very different for ordinary and extraordinary rays as shown in figure 7. As the initial absorption in the poorest crystals, the induced absorption is higher for the ordinary ray, that is

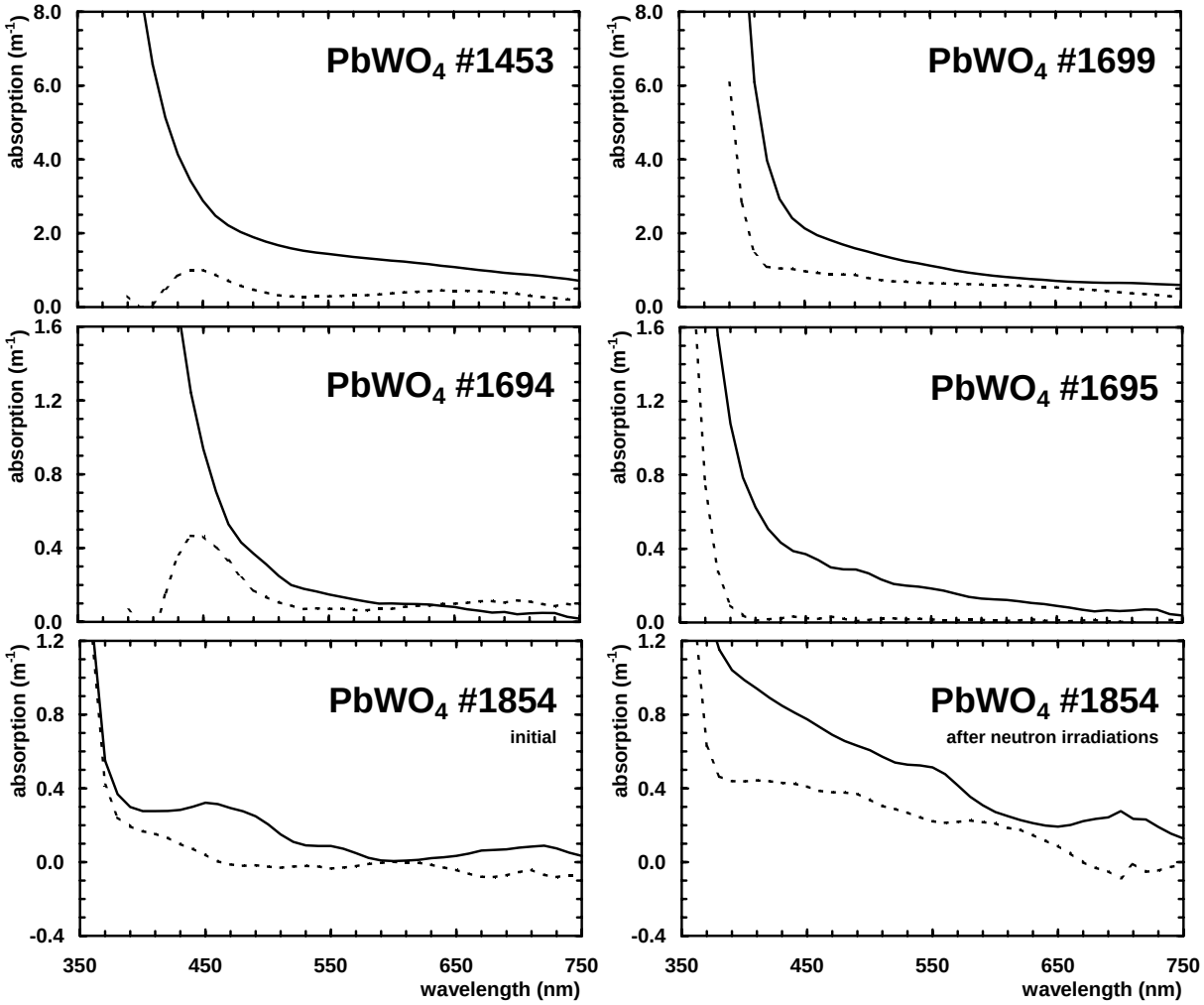

Figure 5: Attenuation coefficients μ_0 (solid line) and μ_θ (dashed line) *versus* wavelength for crystals #1453, #1694, #1695, #1699 and #1854. Notice the differences in scale between crystals.

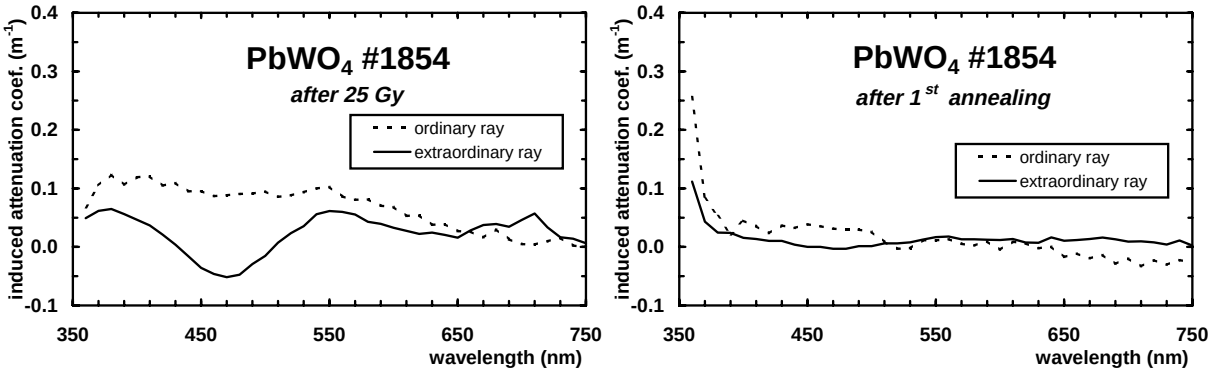

Figure 6: Induced absorption coefficients in crystal #1854 *versus* wavelength for the ordinary and extraordinary rays, after 25 Gy irradiation (left), and annealing (right).

when the light is polarized along the optical axis. A band centred around 520 nm is clearly seen. After annealing the crystal recovered almost its initial transparency. The second neutron irradiation to 2 10^{14} fast neutrons cm^{-2} induced similar results.

4 Conclusion

This study points out the cares that should be taken to perform precise optical absorption characterization of lead tungstate crystals. Strong dependence of absorption on light polarization direction are observed, for the initial absorption in poor crystals, as well as for the induced absorption under radiation in recent, optimised crystals. This behaviour, coupled with the band shape of this absorption, strongly suggests the influence of anisotropic structural defects, such as lead or oxygen vacancy, already invoked for the explanation of radiation resistance variation in these crystals.

However, this absorption dependence takes amplitudes and shapes which depend deeply on the crystal quality and should not be related to one unique type of defect but is rather be a general feature of lead tungstate, besides not astonishing in such strongly anisotropic material.

On a practical point of view, the importance of this effect may imply to incorporate absorption anisotropy (as well as optical anisotropy) in the ray tracing programs, such as LITRANI [14], developed to describe the detector evolution and simulate its ageing.

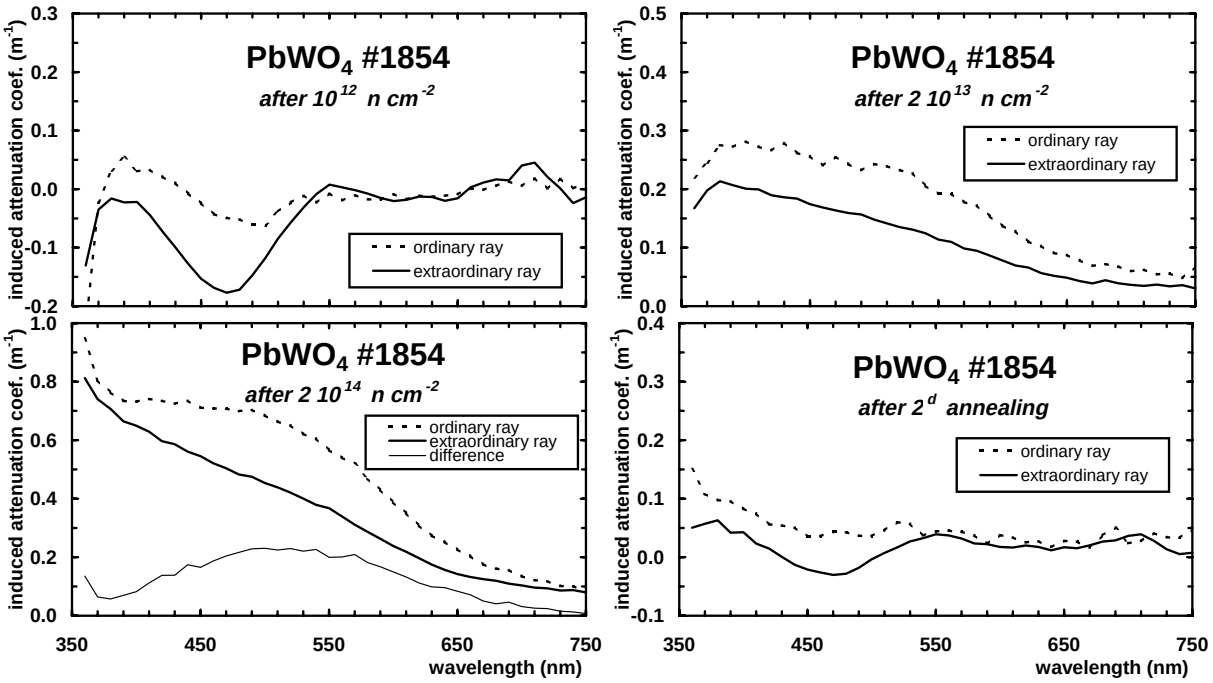

Figure 7: Induced absorption coefficients in crystal #1854 *versus* wavelength for the ordinary and extraordinary rays, after neutron irradiation. Absorption coefficients are calculated comparing transmissions after each irradiation step to before. One must add them to obtain the induced absorption coefficient since the initial state.

Finally the neutron irradiation reported here confirm the early reported [10, 11] long term behaviour of lead tungstate in the CMS calorimeter, with induced absorption lower than 1 m^{-1} after doses equivalent to 10 years of operation, and the improvement of it's short term radiation resistance.

Acknowledgements

This work was in the frame of the CMS ECAL monitoring development project, under the head and with the constant support of J.-P. Pansart and J. Rander. We would like to thanks E. Auffray and P. Lecoq, CERN, wo provided us with up to date crystals. We are indebted, for the neutron irradiation, to J. Safieh, G. Dauphin and the operating team of the Ulysse reactor.

References

[1] CMS collaboration, *"The Compact Muon Solenoid – Technical Proposal"*, CERN/LHCC 94–38, LHCC/P1 (1994).

[2] CMS collaboration, *"The Electromagnetic Calorimeter Project – Technical Design Report"*, CERN/LHCC 97–33, CMS TDR 4 (1997).

[3] J.-M. Moreau, P. Gallez, J.-P. Peigneux and M.V. Korzhik, J. Alloys and Compounds, 238 (1996) 46–48.

[4] M. Lebeau and D. Rinaldi, in : Proc. Int. Conf. on Inorganic Scintillators and their Applications, SCINT 97, Z.W. Yin, P.J. Li, X.Q. Feng and Z.L. Xue eds., CAS Shanghai Branch Press, 1998, p. 230–235.

[5] S. Baccaro et al., Nucl. Instr. and Meth. in Phys. Res. A 385 (1997) 209–214.

[6] S. Baccaro et al., in : Proc. Int. Conf. on Inorganic Scintillators and their Applications, SCINT 95, P. Dorenbos and C.W.E. van Eick eds., Delft University Press, 1996, p. 293–295.

[7] R. Chipaux, *"Numerical formulæ for the refractive index of lead tungstate"*, CMS–TN/95–184 (1995).

[8] Ealing UV-visible linear polarizers, ref. 23–2363.

[9] R. Chipaux, J.-L. Faure, P. Rebourgeard, G. Dauphin and J. Safieh, Nucl. Instr. and Meth. in Phys. Res. A 345 (1994) 440–444.

[10] R. Chipaux et al., in : Scintillator and Phosphor Materials, M.J. Weber, P. Lecoq, R.C. Ruchti, C. Woody, W.M. Yen and R.-Y. Zhu eds. Mat. Res. Soc. Symp. Proc., vol. 358, 1994, p. 481–486.

[11] R. Chipaux and O. Tozon, in : Proc. Int. Conf. on Inorganic Scintillators and their Applications, SCINT 95, P. Dorenbos and C.W.E. van Eick eds., Delft University Press, 1996, p. 274–277.

[12] S. Baccaro et al., Phys. Stat. Sol. (a) 160 (1997) R5.

[13] S. Baccaro et al., Phys. Stat. Sol. (a) 164 (1997) R9.

[14] F.-X. Gentit, *"LITRANI"*,
http://www-dapnia.cea.fr/Spp/Experiences/CMS/cristal/index.htm,
see also :
F.-X. Gentit, *"The Monte-Carlo program Cristal"*, CMS–TN/1996–143 (1996).